Latin American Journal of Solids and Structures
www.lajss.org

Dynamic behaviors of visco-elastic thin-walled spherical shells impact onto a rigid plate

Abstract

As a representative structure, ping-pong balls are usually used to study the mechanical properties of thin-walled spherical shells. In a previous study, the dynamic behaviors of ping-pong balls impinged onto a rigid plate were investigated. It was found that the dynamic deformation energy of the balls could be several times higher than that under quasi-static compression, which could not be completely explained by elastic-plastic material property, strain-rate and inertial effects. In this paper, more impact tests were conducted and the details including the contact time, deformation and rebound behaviors with different impact velocities were reinvestigated. Based on the experimental results, visco-elastic material model is applied and the numerical simulation of thin-walled spherical shells impact onto a plate is performed, in which the influences of the visco-elastic parameters and the impact velocity on the dynamic behaviors are studied. By adjusting the visco-elastic parameters, the contact time, deformation, and the coefficient of restitution agree well with the experimental results.

Keywords

Impact; visco-elastic; coefficient of restitution; spherical shell.

X.W. Zhang*
Z. Tao
Q.M. Zhang

State Key Laboratory of Explosion Science and Technology, Beijing Institute of Technology, Beijing, P.R. China

Corresponding author:
*mezhangxw@bit.edu.cn

Received 05.03.2014
In revised form 14.05.2014
Accepted 13.08.2014
Available online 17.08.2014

1 INTRODUCTION

Due to high load-carrying efficiency and good aerodynamic properties, thin-walled spherical shells are extensively applied not only in engineering structures, but also for sports facilities, such as aircraft, submarine, pressure vessels, oil containers, footballs, tennis balls and so on. Considering loading conditions, their large deformation and buckling behaviors compressed against a rigid plate attract great attentions of researchers.

In earlier decades, theoretical and experimental studies about the deformation modes and contact force of elastic and rigid-plastic spherical shells have been done by Updike and Kalnins (1970; 1972), Kitching et al (1975), De Olivera and Wierzbicki (1982), Gupta et al (1999), most of which focused on the quasi-static cases and the dynamic effects were not considered. To examine the ener-

gy absorption of metal hollow sphere (MHS) materials, Ruan et al (2006) investigated the dynamic crushing of 1D and 2D ping-pong ball arrays under in-plane impacts and found that a single ball's load-deformation relation can be used to predict the ball-array's load deformation behavior. Hubbard and Stronge (2001) conducted the impact tests for ping-pong balls onto a flat plate with velocity 0-20m/s, and obtained the contact time and coefficient of restitution. However, in their analytical modeling, they considered the balls to be pure elastic. As a result, the predictions for the contact time and coefficient of restitution were both higher than the experiments, while the predicted energy dissipation was too little. Besides, Stronge and Achsoft (2007), and Arakawa et al (2007, 2009) studied the impact behaviors of basketballs and golf balls, respectively. Bao and Yu (2012) conducted numerical simulations about the dynamic deformation and rebound behaviors of elastic-plastic balls with different radius/thickness ratios. Cross (2014) measured the contact forces for the ping-pong and squash balls impacting onto a plate.

In a previous study, Zhang and Yu (2012) employed ping-pong balls to study the dynamic buckling behaviors of spherical shells impinged onto a rigid plate by means of air-gun and high-speed camera, and found that even when the impact velocity reached about 45m/s, the deformation of the ball was still recoverable and the dynamic deformation energy of the balls could be several times higher than that under quasi-static compression. Moreover, numerical simulations were also performed by using pure-elastic and elastic-plastic material models. The results revealed that the deformation energy of the ball could not be increased even when the strain-rate effect is considered. By means of energy method, Karagiozova et al (2012) analyzed the influences of inertial effects during the dynamic buckling process of ping-pong balls and pointed out that the local inertia increases the width of the knuckle and the contact force, and that the local vibration of the balls also dissipates some overall kinetic energy. Nevertheless, these effects are still not enough to explain the large enhancement of dynamic deformation energy.

In this paper, to understand the dynamic behaviors of ping-pong ball more clearly, the visco-elasticity of the material is considered. First, more dynamic tests of the ping-pong balls are reported, in which the balls impacted onto smooth and rough plates with impact velocity 4m/s~45m/s, and the contact time, deflection, as well as coefficients of restitution were obtained. Based on the experimental results, the visco-elastic material model is applied to simulate the thin-walled spherical shells numerically and the dynamic process of ping-pong balls is studied. The influences of the visco-elasticity of the materials and impact velocity on the dynamic deformation, contact time and restitution characteristics of the balls are examined.

2 IMPACT TESTS OF THE PING-PONG BALLS

As mentioned above, the previous studies show that with the same deflection, the dynamic deformation energy of the balls was much higher than that in quasi-static cases, and this phenomena could not be explained by pure elastic, elastic-plastic with strain-rate as well as inertial effects. Since the ping-pong balls are made of cellulose which is a typical polymer material, the visco-elasticity of the material must be considered to completely understand the impact behaviors of the ping-pong balls.

For the mechanical properties of ping-pong ball materials, Ruan et al (2006) conducted quasi-static tensile tests for this material, and found that the Young's modulus and yield stress were $E =$

2.4GPa and $\sigma_y = 47$MPa, respectively. Leung and Yu (2008) developed a mini-Split Hopkinson tensile bar and tested the plastic behavior under strain-rate 100-1000 (1/s), but it was not accurate enough to obtain the dynamic modulus of the material. For the measurement of linear visco-elastic parameters of polymer materials, DMA (i.e., dynamic mechanical analysis) method is usually applied (Lakes, 2004). However, considering the contact duration of the ball is less than 1ms and the samples are too small, it is quite difficult to obtain its visco-elastic parameters in this time scale by means of conventional measurements.

In order to study the influences of visco-elasticity on the impact behaviors of ping-pong balls, more experiments were conducted in which the same-brand ping-pong balls were used and the emphasis was placed on the dynamic deformation, rebound behaviors as well as energy dissipation of the balls. The results will be used to evaluate the visco-elastic parameters of the material numerically.

2.1 Description of the experiments

As shown in Figure 1(a), in the experiment, the ping-pong ball were first accelerated by a spring, and then impacted onto a marble plate with a velocity V_0. To record the contact status distinctly, a high-speed camera was aligned with the surface of the plate. The frame rate of the camera was set to 42000 (1/s) so that the time increment of photos was 0.0238ms. Two kinds of friction conditions between the ball and the plate were studied, which were smooth and coarse contacts, respectively. The smooth contact means a naked marble surface was used, while for the coarse contact, a sand paper was pasted tightly on the surface of the plate. By means of friction measurement, the friction coefficient between the plate and the ball for the smooth contact was obtained to be bout 0.3, while that for the coarse contact was larger than 3.

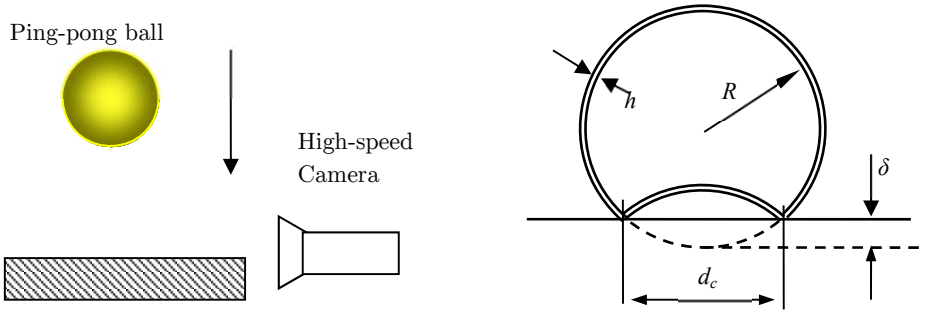

Figure 1: Diagram for the experimental setup and specimen.

As shown in Figure 1(b), the radius and thickness of the ball were measured to be $R = 19.8$mm and $h = 0.38$mm, while the mass of a single ball was $m = 2.67$g. When the velocity of the ball becomes zero, its deflection and contact diameter reach maximum, i.e., δ and d_c, respectively, which could be measured from the pictures.

2.2 Results for the impact tests

The impact tests with initial velocity changing from 4m/s to 45m/s were conducted for both smooth and coarse contact cases. The results for the contact time, deformation and rebound behaviors are listed in Table 1, in which the rebound velocity and contact time are denoted by V_R and t_c, respectively. The coefficient of restitution COR and input energy E_{in} are obtained by

$$COR = \frac{V_R}{V_0},\ E_{in} = \frac{1}{2} m V_0^2 \tag{1}$$

It was found that most of the balls completely recovered when they separated with the plate. However, in test No.13, the ball recovered after it separated with the plate, while for the tests No.14, No. 26 and No.27, the balls were totally unrecoverable even after tests.

No.	V_0/ms^{-1}	V_R/ms^{-1}	t_c/ms	COR	d_c/mm	δ/mm	E_{in}/mJ	contact
1	4.26	4.22	0.50	0.98	9.8	0.7	23.6	S
2	4.13	3.52	0.524	0.850	7.93	0.54	22.2	S
3	10.33	7.60	0.533	0.736	15.2	1.28	138.7	S
4	13.45	9.95	0.633	0.740	18.6	1.65	235.2	S
5	13.13	10.02	0.667	0.763	18.0	2.17	224.1	S
6	13.94	10.8	0.643	0.775	18.1	2.45	252.6	S
7	16.8	11.42	0.69	0.679	20.0	2.80	367.3	S
8	18.3	12.03	0.70	0.66	22.85	3.06	432.9	S
9	21.2	10.91	0.81	0.514	22.27	3.67	584.3	S
10	24.8	10.59	0.90	0.438	24.14	4.22	757.6	S
11	26.57	9.88	1.0	0.372	26.11	5.01	917.8	S
12	27.80	10.24	0.90	0.368	26.11	4.73	1004.7	S
13	31.44	6.89	0.643	0.219	26.33	5.52	1285.0	S
14*	35.19	5.8	0.533	0.165	29.5	6.26	1609.8	S
15	4.75	4.29	0.619	0.903	11.4	0.465	29.3	C
16	7.10	5.32	0.619	0.749	13.87	0.867	65.5	C
17	11.45	8.34	0.643	0.728	17.89	1.49	170.4	C
18	15.04	9.87	0.643	0.656	18.95	1.93	294.1	C
19	16.96	10.87	0.738	0.641	20.93	2.83	373.9	C
20	18.37	11.29	0.738	0.615	22.29	3.48	438.7	C
21	25.8	11.11	0.881	0.431	26.6	4.52	865.3	C
22	27.48	13.37	0.786	0.487	24.68	4.64	981.7	C
23	28.07	11.1	0.81	0.395	25.99	4.52	1024.3	C
24	35.55	11.28	0.952	0.317	28.49	6.07	1642.9	C
25	36.45	9.59	1.07	0.263	27.53	5.64	1727.2	C
26*	40.43	6.85	0.785	0.169	28.73	7.25	2125.0	C
27*	45.34	5.86	0.69	0.129	29.78	6.73	2672.4	C

Note: the superscript '*' means the deformation was unrecoverable, while for the contact, 'S' and 'C' are smooth and coarse, respectively.

Table 1: Experimental results for the impact tests.

Figure 2 shows the deformation and contact status of the ball at some representative moments for the smooth contact test with $V_0 = 21.2$m/s. It can be seen that at $t = 0$, the ball didn't contact the plate, while at $t = 0.0238$ms, they began to contact with each other. At $t = 0.3332$ms, the deflection of the ball reached maximum. After that, the ball rebounded and they separated at $t = 0.857$ms. Therefore, the contact time for this test was about 0.833ms. From the pictures, the maximum contact diameter and deflection are found to be 22.3mm and 3.67mm, respectively. Also, the rebound velocity was 10.91m/s, which means that the coefficient of restitution was 0.514.

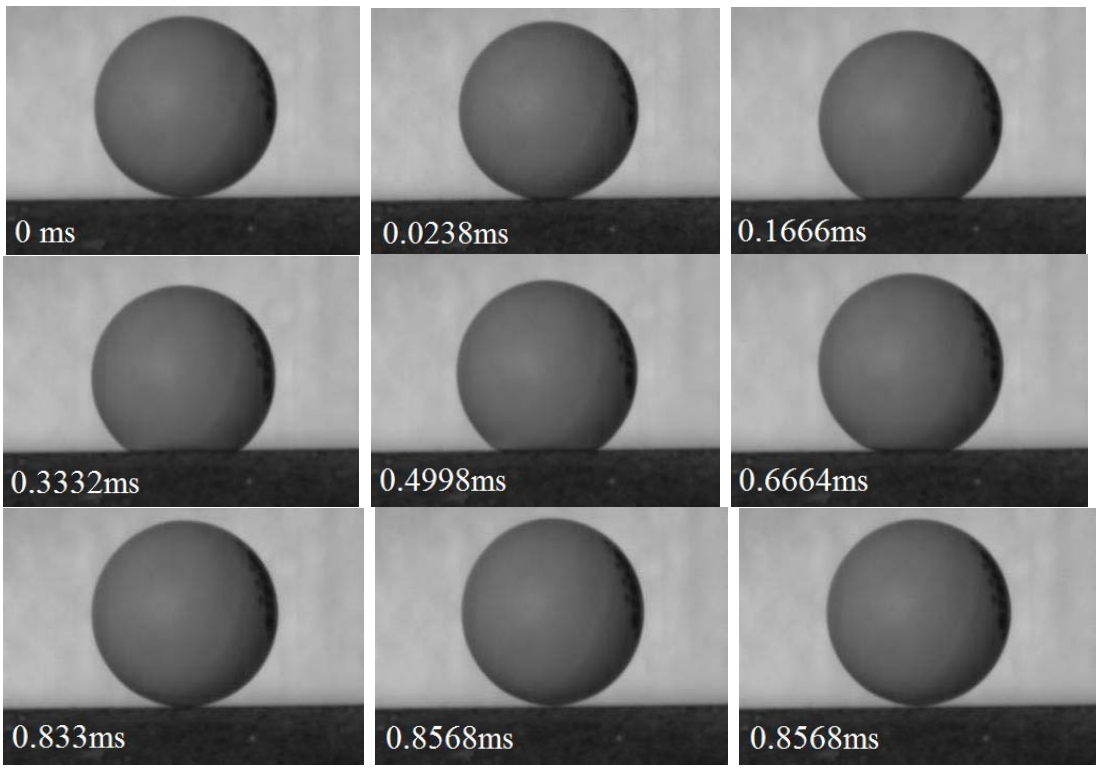

Figure 2: Typical frames for the test with smooth contact and $V_0 = 21.2$m/s.

The relation between the contact time and impact velocity is plotted in Figure 3(a), which shows that for $V_0 < 30$m/s, t_c increases with the increase of V_0. When V_0 is about 5m/s, t_c is between 0.5ms and 0.6ms, but for $V_0 = 30$m/s, it reaches about 0.8~1.0ms. It should be pointed out that for the cases with $V_0 < 2$m/s, Hubbard and Stronge (2001) measured the contact time which increases with the decrease of the impact velocity. It can be seen that when the impact velocity is lower than 20m/s, t_c for smooth contact is a little lower than that for coarse contact. However, after that, it gradually becomes even larger. Moreover, it is found that for the smooth contact tests, the contact time t_c suddenly dropped when $V_0 > 30$m/s, which is because the deformation was not recovered on time. The case is similar for the coarse contact tests after $V_0 > 35$m/s.

The coefficient of restitutions for different impact tests are shown in Figure 3(b). It reveals that *COR* decreases almost linearly with the increase of V_0. When the impact velocity is lower than 20 m/s, the *COR* for smooth contact is higher than that for coarse contact. However, when V_0 is close

to 30m/s, it reverses, which is due to the unrecoverable deformation for smooth contact while it is still recoverable for coarse contact cases.

When the deflection and contact diameter of the ball reach maximum, most of the input kinetic energy transfers to the deformation energy, with only a small part going to the vibration of the ball. Figure 4(a) shows the relation between the input energy and the maximum deflection of the ball. For comparison, the quasi-static result for the relationship between the deformation energy and deflection is also plotted. It is shown that with the same deflection, the dynamic deformation energy of the ball is about 2.5~3 times of that in quasi-static test and no distinct difference between the smooth contact and coarse contact tests is found.

Figure 4(b) plots the experimental results for the input energy at different maximum contact diameter, which shows that at the same contact diameter, the input energy is much higher than the deformation energy in quasi-static test. It should be pointed out that when the maximum contact diameter is close to 28mm, the dynamic deformation of the ball is still recoverable. However, in the quasi-static compression test, the deformation of the ball was unrecoverable when d_c was larger than 22mm.

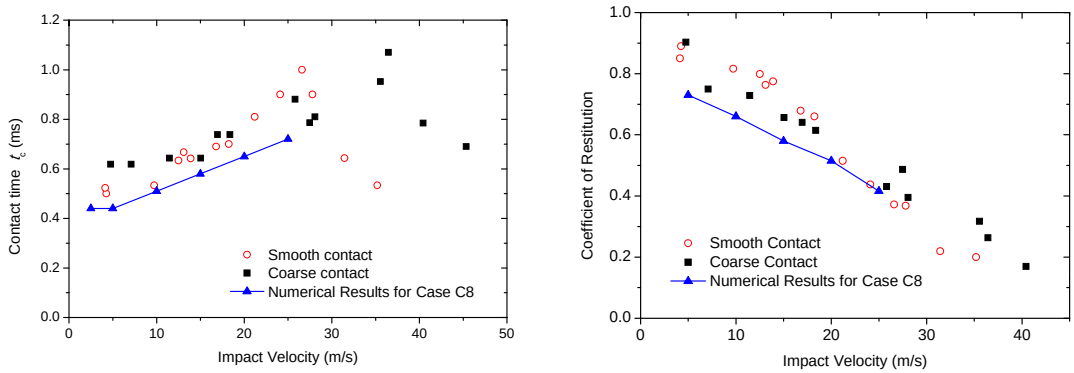

(a) (b)

Figure 3: Experimental results for contact time and coefficient restitution: (a) Contact time; (b) Coefficient of restitution.

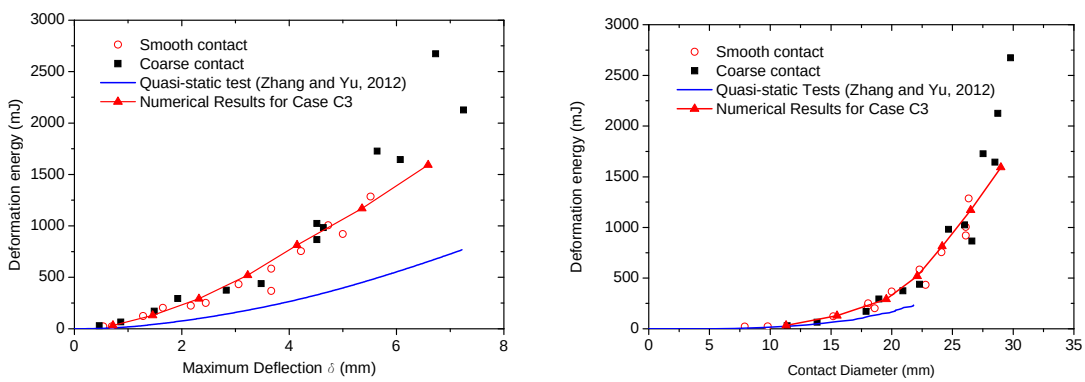

(a) (b)

Figure 4: Experimental results for deformation: (a) input kinetic energy v.s. maximum deflection of the ball; (b) input kinetic energy v.s. the contact diameter.

3 NUMERICAL SIMULATIONS

To dig out more details about the dynamic behaviors of the ping-pong ball and study the influences of the visco-elasticity, the impact process of visco-elastic thin-walled spherical shells is simulated by means of non-linear finite element code ABAQUS/ explicit.

3.1 Definition of the visco-elastic materials

For visco-elastic materials, generalized Maxwell models are extensively used to study the mechanical properties of biological soft tissues and polymer materials (Zhang, et al, 2007; Wu et al, 2007). As shown in Figure 5, a generalized Maxwell model is composed of a spring element with elastic modulus E_0 and n Maxwell elements (i.e., spring-dashpot) in parallel. The elastic modulus and viscous coefficient of the i th Maxwell element are E_i and η_i, respectively. Then, the differential constitutive equation of this model can be expressed by (Lakes, 1998)

$$p_0\sigma + p_1\dot{\sigma} + p_2\ddot{\sigma} + \cdots = q_0\varepsilon + q_1\dot{\varepsilon} + q_2\ddot{\varepsilon} + ... \tag{2}$$

where p_i and q_i are functions of E_i and η_i, with $i = 0, 1, 2... n$.

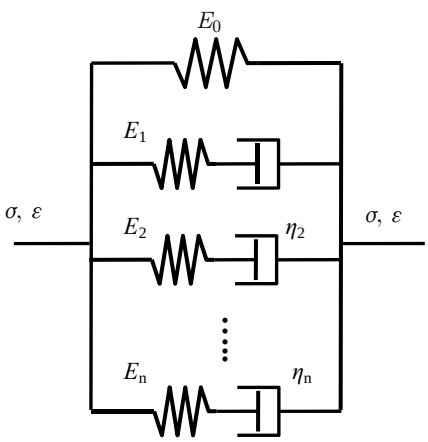

Figure 5: Diagram for the generalized Maxwell model.

In ABAQUS, the visco-elasticity of material can be defined based on creep or stress relaxation tests. For small strain, the shear stress of the visco-elastic material is

$$\tau(t) = \int_0^t G_R\left(t-s\right)\dot{\gamma}\left(s\right)ds \tag{3}$$

where $G_R\left(t\right)$ is the time-dependent shear relaxation modulus. This constitutive behavior can be obtained by relaxation tests. For given initial strain γ, the shear stress during the relaxation test is

$$\tau(t) = G_R(t)\gamma \tag{4}$$

If denote the dynamic shear modulus $G_d = G_R(0)$, the instantaneous shear modulus can be non-dimensionalized by

$$g(t) = G_R(t) / G_d \tag{5}$$

When t is infinite, its shear modulus $G_R(\infty)$ equals to the quasi-static shear modulus G_0. Therefore, the visco-elastic properties can be defined by G_0 and $g(t)$. Usually, $g(t)$ is expressed in the following form (Lakes, 1998)

$$g(t) = 1 - \sum_{i=1}^{n} g_i(1 - e^{-t/\theta_i}) \tag{6}$$

By giving n, q_i and θ_i, the shear visco-elastic behavior can be defined. On the other hand, the volumetric behaviors of the material can be defined in the same way. Assuming they conform to the same constitutive model as shown in Figure 5, then the visco-elastic parameters are

$$g_i = \frac{E_i}{E_d},\ \theta_i = \frac{\eta_i}{E_i},\ E_d = E_0 + \sum_{i=1}^{N} E_i \quad i = 1,2 \ldots n \tag{7}$$

where E_d is the dynamic elastic modulus of the material.

In order to simulate the visco-elastic behaviors of real materials more vividly, a large number of Maxwell elements with various characteristic frequencies are needed. However, the parameters of the elements are not easy to be obtained. Most studies just considered the hysteresis, creep and stress relaxation behaviors which last a long time, while few concern about the impact responses of visco-elastic materials. Usually one or two Maxwell models are enough to describe the impact response. For example, a weak nonlinear visco-elastic model was proposed (Wang. et al, 2008) for describing the dynamic behaviors of polymers in a wide range of strain rate, which was composed of a nonlinear spring and two viscous-elastic elements.

3.2 Modeling of the impact process

According to previous studies (Ruan, et al, 2006; Zhang and Yu, 2012), the elastic modulus and yield stress of the ping-pong balls material are 2.4GPa and 47MPa, respectively, and its density is 1.4g/cm^3. Since the radius/ thickness ratio of the balls is larger than 100, shell elements SR4 with five integration points through the thickness are used for modeling the ball and the plate is defined as a rigid body. During the impact process, the plate is fixed and the ball impacts it with an initial velocity V_0. The contact between the two bodies is defined by penalty method with the friction coefficient μ. It should be pointed out that in the real situation, the internal pressure will increase due to the deformation of the ball. However, even when the maximum deflection of the ball is $\delta = 0.4R$, the change of the internal pressure is about 10%. Therefore, for simplicity, only constant internal pressure p is considered. As shown in Figure 6, the mesh near the contact area between the ball and the plate is denser than the other area. The total number of elements is 4795.

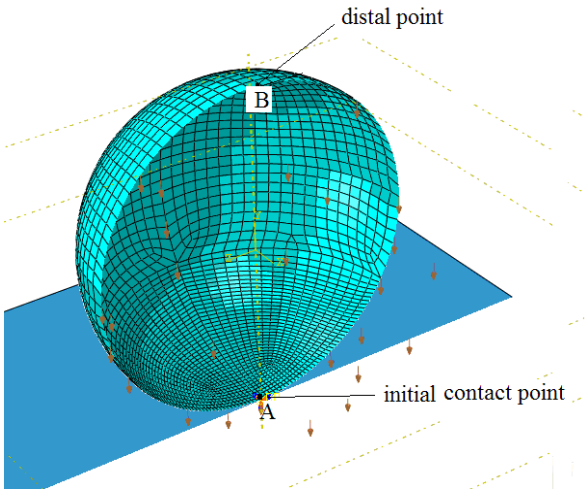

Figure 6: Half part of the FEM model of a ping-pong ball.

Considering in the impact tests the deformation of the balls was almost recoverable, the material is assumed to be visco-elastic and its yield stress is ignored. Since the visco-elastic properties of the material are unknown, according to its quasi-static elastic modulus $E_0 = 2.4\text{GPa}$ and the impact test results, a series of combinations of the visco-elastic parameters, i.e., g_i and θ_i, are trailed in the simulations and the numerical results are compared with the experiments to obtain a relatively good one. At the same time, the influences of visco-elastic parameters on the dynamic responses are analyzed. To simplify the numerical study, at most two Maxwell elements are used. Moreover, other factors, i.e., friction coefficient μ and the internal pressure p, are also considered and their influences on the deformation, contact time as well as the coefficient of restitution are studied.

4 NUMERICAL RESULTS AND DISCUSSIONS

4.1 Impact response of the balls

According to the impact tests, the dynamic deformation energy is about 2.5~3 times of that in the quasi-static case. Therefore, the visco-elastic parameter combination with $g_1 = g_2 = 0.33$ (i.e., $E_d = 7.2\text{GPa}$), $\theta_1 = 10\text{ms}$ and $\theta_2 = 1\text{ms}$ is first employed, which is denoted as case C1. The impact process with $V_0 = 25\text{m/s}$, $p = 0$, $\mu = 0.3$ is simulated.

The velocity and displacement of the initial contact point A and distal point B (as shown in Figure 6) are plotted in Figure 7 (a) and (b). Since the deformation of the balls mainly occurs near the contact region, the displacement of the distal point could represent the movement of the ball. It can be seen that after contact, the velocity of the ball gradually decreases from V_0 to zero and then it rebounds. On the other hand, at the contact moment, the velocity of point A suddenly drops to zero and then gradually increases in the opposite direction with small vibrations.

At $t = 0.05\text{ms}$, its velocity sharply reaches about 40m/s, which is nearly two times of V_0, revealing that at this moment, the snap-through of the contact region occurs. It should be pointed out

that, although before $t = 0.05$ms the contact point departs from the plate, it is not the real snap-through but due to the stress wave propagation. This phenomenon can also be found in displacement-time curves in Figure 7(b), which shows that before $t = 0.05$ms, the displacement of contact point increases relatively slowly. Then, the velocity of the contact point accelerates in the opposite direction and at $t = 0.58$ms it becomes larger than 40m/s. However, at this moment, its velocity suddenly reverses to 20m/s in the same direction with that of the distal point, which is due to the wave propagation in the structure. After that, the velocities and displacements of the two points reach the same the value, and the ball separates with the plate. The contact time of this impact process is found to be 0.62ms.

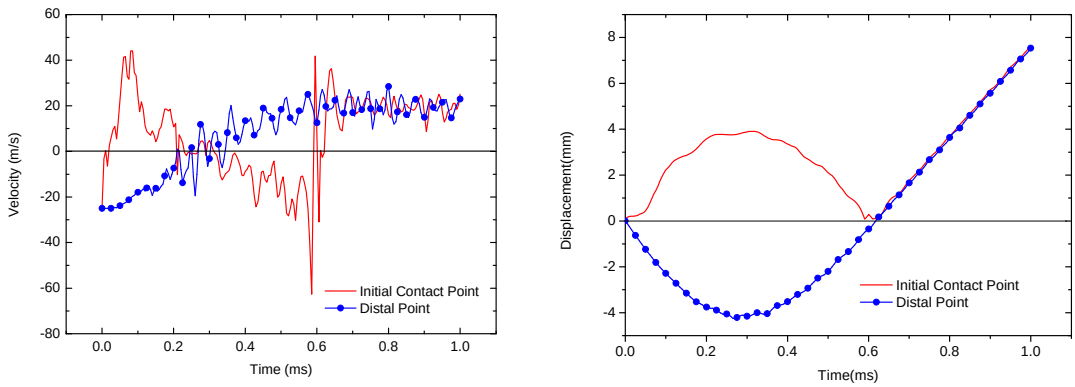

(a) (b)

Figure 7: Numerical results for case C1 with $V_0 = 25$m/s: (a) velocity; (b) displacement.

The rebound velocity of the ball can be obtained by averaging the velocity or calculating the slope of the displacement curves after separation. It can be obtained as $V_R = 20.5$m/s so that the coefficient of restitution of this numerical case is COR=0.80.

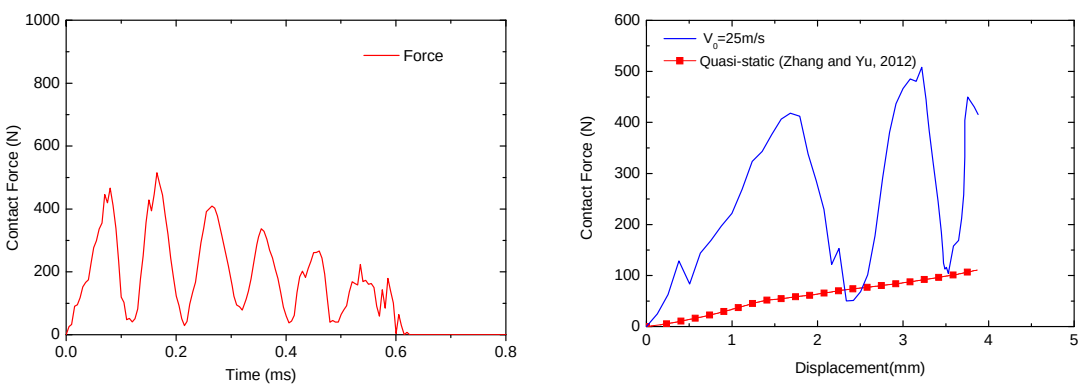

(a) (b)

Figure 8: Contact forces for the numerical case C1 with $V_0 = 25$m/s: (a) force history; (b) force-displacement relationship.

The history of the contact force between the ball and the plate is shown in Figure 8(a). It can be seen that after they contact each other, the contact force increased from zero with serious fluctuations. At around $t = 0.17$ms, the contact force reach its maximum, which is about 515N. Then, it gradually decreases. At $t = 0.62$ms, the contact force becomes zero and the ball departs from the plate. The contact force with respect to displacement of the ball during the inbound stage is plotted in Figure 8(b). Compared with the quasi-static result, the dynamic force is greatly increased. However, due to the force fluctuation, the maximum contact force doesn't occur at the maximum deflection. Besides, for this impact case, the maximum contact diameter and deflection are found to be 23.9mm and 4.01mm, respectively.

Cases No	Visco-elastic parameters					Results			
	E_0/GPa	g_1	g_2	ϑ_1/ms	ϑ_2/ms	t_c/ms	COR	d_c/mm	δ/mm
Exp	--	--	--	--	--	0.8~0.9	0.43	24.14	4.22
C1	2.4	0.33	0.33	10	1.0	0.62	0.80	23.9	4.01
C2	7.2	0	0	0	0	0.55	0.90	23.7	3.98
C3	6.4	0	0	0	0	0.60	0.90	24.7	4.27
C4	2.4	0.625	0	1	0	0.62	0.743	24.15	4.20
C5	2.4	0.625	0	0.4	0	0.69	0.515	24.15	4.14
C6	2.4	0.6	0.025	0.4	0.1	0.70	0.467	24.15	4.15
C7	2.4	0.58	0.045	0.4	0.1	0.72	0.44	24.15	4.15
C8	2.4	0.57	0.055	0.4	0.1	0.72	0.42	24.15	4.15

Note: the results for case 'Exp' are from the test No. 10 with $V_0 = 24.8$m/s

Table 2: Comparison between the experimental and numerical results for V_0=25m/s.

The comparisons between the experimental results and some typical simulation cases for $V_0 = 25$m/s are listed in Table 2. It can be seen that the maximum deformation of the ball obtained by the case C1 is relatively close to the experimental result, but the contact time and coefficient of restitution don't agree with the experiments. Therefore, to obtain acceptable visco-elastic parameters for the ball material, their influences on the deformation, contact time and restitution behaviors are studied in the following sections.

4.2 Dynamic deformation of the ball

By using $E_0 = 7.2$GPa, the impact process of a pure elastic ball with $V_0 = 25$m/s is simulated, which is noted by case C2. As shown in Table 2, the differences of the deformation results (i.e., d_c and δ) between cases C1 and C2 are small, but the contact time and restitution coefficient are quite different, which means that the dynamic deformation of the ball is mainly determined by the dynamic elastic modulus, while the influences of relaxation time are relatively weak.

To analyze the inertial effect, the relations between the contact force and the displacement of the ball for pure elastic cases with $E_0 = 2.4$GPa are plotted in Figure 9(a). It can be seen that the dynamic contact force has great fluctuations. For $V_0 = 10$m/s, there are two peak forces and the second peak is maximum. For $V_0 = 20$m/s and 30m/s, between two peak forces, there is a period at which the dynamic contact force is zero, which reveals that for large impact velocities, the impact response is a multi-contact process. Although, in the ascending stage of the first peak, the dynamic

forces are greatly higher than the quasi-static contact force, considering the serious fluctuations, when the deflection reaches maximum, the dynamic deformation energy doesn't increase much compared with the quasi-static deformation energy at the same deflection. Therefore, the influence of the inertial effect on the dynamic deformation energy of the ball is not distinct.

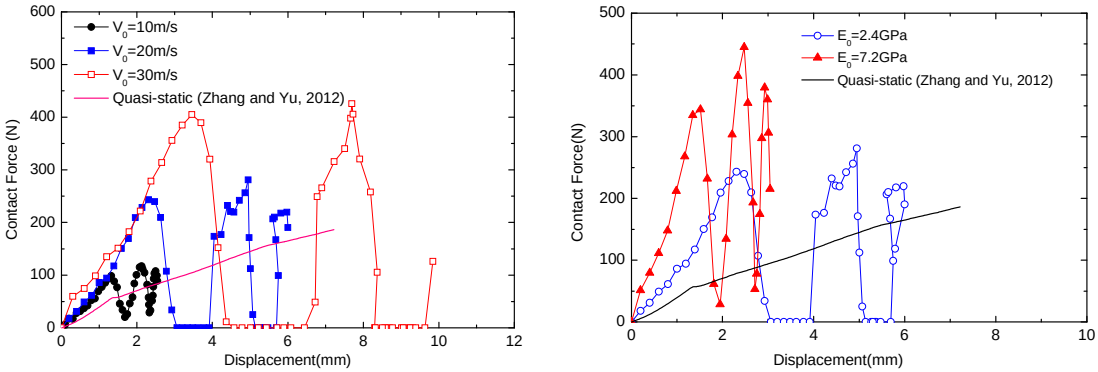

(a) (b)

Figure 9: Numerical results for pure elastic cases:
(a) for $E_0 = 2.4\text{GPa}$ with different V_0; (b) for $V_0 = 20\text{m/s}$ with different E_0.

The contact forces for the cases with elastic modulus $E_0 = 2.4\text{GPa}$ and 7.2GPa at $V_0 = 20\text{m/s}$ are also compared in Figure 9(b), which shows that for the same input kinetic energy, the ball with larger elastic modulus will have higher contact force and smaller maximum deflection. Therefore, the great increase of the dynamic deformation energy of the ball is mainly due to the dynamic elastic modulus of the material.

To seek a suitable dynamic elastic modulus for the ball, pure elastic cases with $E_0 = 5\tilde{}12\text{GPa}$ and $V_0 = 25\text{m/s}$ are investigated. It is found that the deformation for the case with $E_0 = 6.4\text{GPa}$ agrees well with the experiment, which is shown in Table 2 as case C3. By keeping $E_0 = 6.4\text{GPa}$, the impact process for different impact velocities are simulated. The numerical results for the relations between the input kinetic energy and the maximum deflection and contact diameter of the ball are compared with the experiments in Figure 4(a) and (b). It is found that, the results for $E_0 = 6.4\text{GPa}$ agree well with the impact tests results. Therefore, $E_d = 6.4\text{GPa}$ is an acceptable dynamic modulus for the ball material, i.e., $g_1 + g_2 = 0.625$. However, the specified values of g_i as well as the corresponding relaxation times θ_i still need to be determined by the contact time and restitution coefficient analysis.

4.3 The contact time

Obviously, the contact time of an elastic thin-walled spherical shell is mainly determined by its mass and elastic stiffness which is similar to a mass-spring system. However, in this section, only the influences of the visco-elasticity of the material are considered. For simplicity, one Maxwell element is first employed to examine the influences of the relaxation time on the contact time. The dynamic elastic modulus $E_d = 6.4\text{GPa}$ (i.e., $E_0 = 2.4\text{GPa}$, $g_1 = 0.625$) and the relaxation time $\theta_1 = 0.1\text{ms}\tilde{}10\text{ms}$ are studied.

The numerical results for $V_0 = 25\text{m/s}$ are plotted in Figure 10, which shows that when θ_1 changes from 10ms to 2ms, the contact time increases very slowly. When θ_1 is smaller than 2.0ms, the influence of relaxation time becomes remarkable. For $\theta_1 = 0.4\text{ms}$, the contact time is $t_c = 0.69\text{ms}$ as shown in Table 2 noted by C5. However, it is found that when $\theta_1 < 0.4\text{ms}$, the contact time suddenly drops to about 0.4ms, which is because the deformation of the ball doesn't completely recover before it departs from the plate.

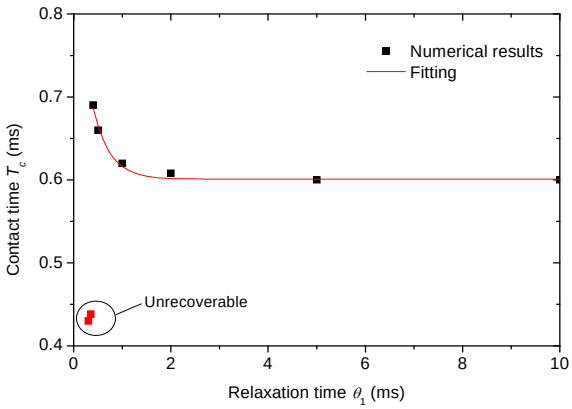

Figure 10: Influences of the relaxation time for one-Maxwell-element model with $E_0 = 2.4\text{GPa}$, $g_1 = 0.625$ and $V_0 = 25\text{m/s}$.

Since the experimental contact time is about 0.8ms~0.9ms, to get even closer numerical result, the visco-elastic model with two Maxwell elements is considered. Considering that there are too many parameters that could be adjusted, for convenience, several combinations of viso-elastic parameters are trialed by keeping $E_d = 6.4\text{GPa}$ (i.e., $E_0 = 2.4\text{GPa}$, $\Sigma g_i = 0.625$), $\theta_1 = 0.4\text{ms}$ and $\theta_2 = 0.1\text{ms}$.

Some typical results are listed in Table 2 as C6-C8. It is found that the increase of g_2 will cause the increase of the contact time. However, when g_2 is larger than 0.055, the ball cannot totally recover before it departs from the plate. With the visco-elastic parameters combination C8, the contact time is about 0.72ms. It should be pointed out that, although the result for this group of parameters is still a little lower than the experimental result, further improvement by adjusting the parameters based on the two-Maxwell-element model is very limited.

The contact times for numerical case C8 with different impact velocities are plotted and compared with the experimental results in Figure 3 (a). It can be found that when the impact velocity increases from 5-25m/s, the impact time changes from 0.44ms to 0.72ms. Although the contact times are a little lower than the experiments, considering the error of experiments, they are still acceptable.

With the visco-elastic parameters in C8, the impact processes for $V_0 = 10\text{m/s}$ and 25m/s with different friction coefficients and internal pressures are simulated and the results are shown in Figure 11(a) and 11(b). It is found that when μ increases from 0 to 1.0, the change of contact time is not distinct. However, when the internal pressure increases from 0 to 0.2MPa, the contact time decreases distinctly.

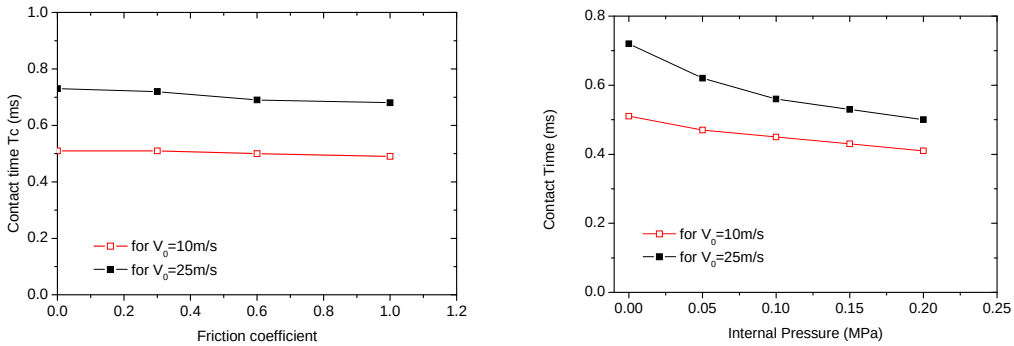

(a) (b)

Figure 11: Influences of the friction and internal pressure on the contact time for the case C8: (a) friction coefficient; (b) internal pressure.

4.4 Rebound and restitution behaviors

First, the influence of the impact velocity on *COR* is studied, in which both pure elastic and visco-elastic cases are considered. As shown in Figure 12(a), for $V_0 = 2.5$m/s, the *COR*s for pure elastic cases with $E_0 = 2.4$GPa and 7.2GPa have nearly no difference, which are 0.99. With the increase of V_0, the *COR* decreases almost linearly. And, for the same impact velocity, the smaller the elastic modulus, the smaller the *COR* will be. The results for the case C8 are plotted in Figure 12(a) and also compared with the experiments in Figure 3 (b). It is seen that at $V_0 = 2.5$m/s, the result for C8 is about 0.80, which is lower than the experiment. However, when the impact velocity is close to 25m/s, the *COR*s have good agreement with the dynamic experiments.

In Figure 12(b), the influence of the relaxation time is examined. For convenience, only one damping element is considered, in which $E_d = 6.4$GPa and the relaxation θ_1 is between 0.1-10ms. It can be found that when the relaxation time is lower than 2ms, the decrease of the relaxation time will induce great decrease of *COR*. However, for the case $\theta_1 > 2$ms, the change of *COR* becomes very smooth. This is because the contact time is only about 0.6-0.7ms so that the elastic strain energy has not been released much for the cases with larger θ_1.

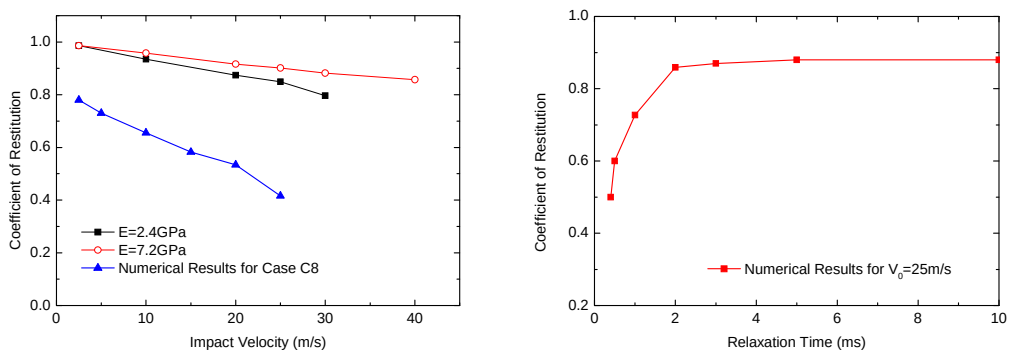

(a) (b)

Figure 12: Influences of impact velocity and relaxation time on the *COR*: (a) Impact velocity; (b) relaxation time.

Moreover, the influences of the friction coefficient and internal pressure are studied and the results for $V_0 = 10\text{m/s}$ and 25m/s with the material parameters C8 are plotted in Figure 13(a) and (b). It is shown that with the increase of the friction coefficient, the *COR* decreases for $V_0 = 10\text{m/s}$, but it increases for $V_0 = 25\text{m/s}$. After analyzing, the friction has two effects, which are dissipation of the energy and increase of the contact rigidity. The simulation results show that the former effect is dominant when the impact velocity is low, while for high velocity impact, the friction will increase the contact rigidity so that the *COR* increases and the contact time decreases. On the other hand, the internal pressure will directly increase the rigidity of the ball and increase the *COR* as shown in Figure 13(b). Therefore, the *COR* of a ball can be improved by inflation.

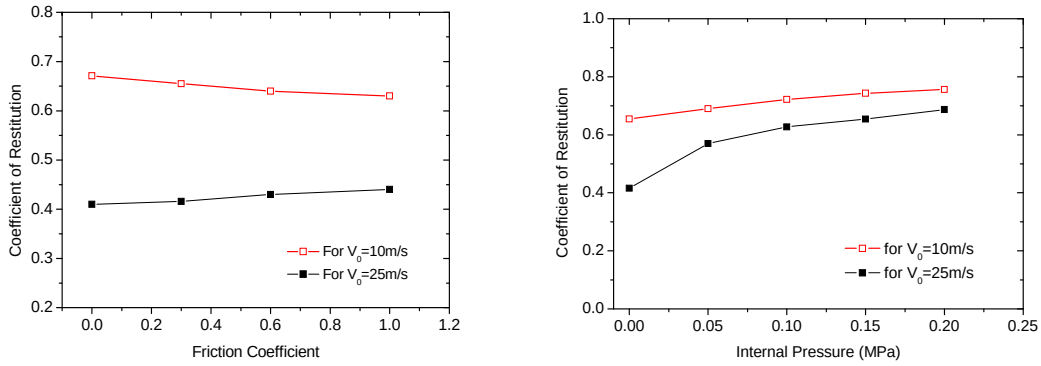

(a) (b)

Figure 13: Influences of the friction and internal pressure on the *COR* for the case C8: (a) the friction coefficient; (b) internal pressure.

5 CONCLUDING REMARKS

In order to clarify the large enhancement of dynamic deformation energy of ping-pong balls impacting onto a rigid plate found in a previous study, a series of more systematic impact tests were first conducted in which the dynamic deformation, contact time as well as coefficient of restitution at different impact velocities were obtained. It is found that for given maximum contact diameter or deflection, the input kinetic energy in the impact scenario was about 2.5~3 times of the deformation energy in quasi-static compression test, and with the increase of impact velocity, the contact time increases while the coefficient of restitution decreased almost linearly.

Based on the experiments, the impact process is numerically simulated by means of visco-elastic material model and the influences of the material properties are analyzed. The results show that under the impact scenarios, the dynamic deformation energy of the ball is mainly determined by the dynamic elastic modulus of the material, while the influence of the relaxation time is relatively weak. The contact time and coefficient of restitution not only depend on the dynamic elastic modulus, but also on the relaxation time. With the decrease of the relaxation time, the contact time increases and the coefficient of restitution decreases. However, if the relaxation time is far larger than the contact time, its influence can be ignored. When it is close to or smaller than the contact time, this influence becomes remarkable. It is also found that when the relaxation time is too small, the defor-

mation cannot recover completely before the ball departs from the plate. Besides, with the same visco-elastic parameters, the influence of the friction coefficient is not very distinct, while the internal pressure will cause the decrease of the contact time and increase of the coefficient of restitution.

After trying a series of visco-elastic parameter combinations, a group of visco-elastic parameters for the generalized Maxwell model with two spring-dashpot elements is obtained, by means of which the dynamic deformation, contact time and the coefficient of restitution of the ping-pong ball at different impact velocities have good agreement with the experimental results. Since this group of visco-elastic parameters are obtained based on the simulations for $V_0 = 25\mathrm{m/s}$, the results still have some relatively larger differences for other velocities, which may be due to the nonlinear visco-elasticity of the material. Anyhow, this study shows that for the structures made of polymer materials under impact loadings, the visco-elasticity must be considered to obtain correct dynamic responses. For more accurate analysis, the visco-elastic properties of the ball material in impact scenarios are expected to be characterized in the future study.

Acknowledgements

This study is funded by the National Natural Science Foundation of China with Project No.11102025 and the State Key Laboratory of Explosive Science and Technology under the Project No.QNKT11-03. Their financial supports are gratefully acknowledged.

References

Arkawa, K., Mada, T., Komatsu, H., et al, (2007). Dynamic contact behaviors of a golf ball during oblique impact: effect of friction between the ball and target. Experimental Mechanics 47(2): 277-282.

Arakawa, K., Mada, T., Komatsu, H., et al, (2009). Dynamic deformation behaviors of a golf ball during normal impact. Experimental Mechanics 49(4): 471-477.

Bao, R., Yu, T.X., (2013). Impact Crushing and rebound of thin-walled hollow spheres, Key engineering materials 535-536: 40-43.

Cross, R., (2014). Impact behavior of hollow balls. American Journal of Physcis 82(3): 189-195.

De Oliveira, J.G., Wierzbicki, T., (1982). Crushing analysis of rotationally symmetric plastic shells. Journal of strain analysis 17(4): 229-236.

Gupta, N.K., Easwara, P.G.L, Gupta, S.K., (1999). Axial compression of metallic spherical shells between rigid plates. Thin-walled Structures 34(1): 21-41.

Hubbard, M., Strong, W.J., (2001). Bounce of hollow balls on flat surfaces. Sports Engineering 4(1): 1-13.

Karagiozova, D., Zhang, X.W., Yu, T.X., (2012). Static and dynamic snap-through behavior of an elastic spherical shell, Acta Mechanica Sinica 28(3): 695-710.

Kitching, R., Houlston, R., Johnson, W., (1975). A theoretical and Experimental study of hemispherical shells subjected to axial loads between flat plates. Int. J. Mech. Sci. 17(11-12): 693-703.

Lakes, R.S., (1998). Viscoelastic Solids, CRC press.

Lakes, R.S., (2004). Viscoelastic measurement techniques, Review of Scientific Instruments 75(4): 797-810.

Leung, M.Y., Yu, T.X., (2008). Dynamic characterization of micro-scale samples using Hopkinson tensile bar technique, J. Strain Analysis 43(7): 595-607.

Ruan, H.H., Gao, Z.Y., Yu, T.X., (2006). Crushing of thin-walled spheres and sphere arrays. International Journal of Mechanical Sciences 48(2): 117-133.

Stronge, W.J., Ashcrof, A.D.C., (2007). Oblique impact of inflated balls at large deflections. International Journal of Impact Engineering 34 (6): 1003-1019.

Updike, D.P., Kalnins, A., (1970). Axisymmetric behavior of an elastic spherical shell compressed between rigid plates. Journal of Applied Mechanics 9: 635-640.

Updike, D.P., Kalnins, A., (1972). Axisymmetric postbuckling and nonsymmetric buckling of a spherical shell compressed between rigid plates. Journal of Applied Mechanics 3: 172-178.

Wang, L., Yang, L., Huang, S., Zhang, Z., Chen, G., (2008). An impact dynamics analysis on a new crashworthy device against ship-bridge collision, Int. J. Impact Engng. 35(8): 895-904.

Wu, X., Levenston, M.E., Chaikof, E.L., (2007). A constitutive model for protein-based materials, Biomaterials 27(30): 5315-5325.

Zhang, W., Chen, H.Y., Kassab, G.S., (2007). A rate-insensitive linear visco-elastic model for soft tissues, Biomaterials 28(24): 3579-3586.

Zhang, X.W., Yu, T.X., (2012). Experimental and numerical study on the dynamic buckling of ping-pong balls under impact loading, Int. J. Nonlinear Sci. Numer. Simul. 13(1): 81-92.